

## Krill Oil Quantification in CS/TPP Nanoparticles Using Novel One Step Fourier Transform Infrared Spectroscopy

Junaid Haider<sup>a</sup>, Hamid Majeed<sup>a</sup>, Hafiz Rizwan Sharif<sup>a</sup>, Muhammad Shamoona<sup>a</sup>,  
Haroon Jamshaid Qazi<sup>b</sup>, Ali Haider<sup>c</sup>, Jianguo Ma<sup>a</sup>, Fang Zhong<sup>\*a</sup>

<sup>a</sup>State Key Laboratory of Food Science and Technology, School of Food Science and Technology, Jiangnan University, Wuxi 214122, Jiangsu, P.R China.

<sup>b</sup>Department of Food Science and Human Nutrition, University of Veterinary and Animal Sciences, Lahore, Pakistan.

<sup>c</sup>Department of Clinical Medicine and Surgery, University of Veterinary and Animal Sciences, Lahore, Pakistan.

\*Correspondence author: (Fang Zhong; E-mail: [fzhong@jiangnan.edu.cn](mailto:fzhong@jiangnan.edu.cn))

**ABSTRACT:** Recent success in quantitative analysis of essential fatty acid compositions in encapsulated Krill oil (KO) supplement, we extended the application of Fourier transform infrared spectroscopic technique for rapid determination of KO loading efficiency from the intact biodegradable CS/TPP nanoparticles. Beer-Lambert law was applied in the quantification following selection of a few wave number combinations. The optimized spectral region to attain linear calibration curve for KO/CS-TPP nanoparticles with regression coefficient of  $R^2=0.9959$  for determination of KO. The result revealed successful encapsulation of KO in CS/TPP nanoparticles with loading efficiency of  $22.2 \pm 0.26$  %. Further, to validate the FTIR method for KO contents analysis, gravimetric method was compared that confirmed the same quantity of KO. This method is fast and easy to apply and does not require sample processing. Therefore, current findings confirmed the advantage of FTIR technique in quantification of KO and other bioactive constituents directly and efficiently with no extra sample preparation procedures.

**Keywords:** Krill oil, CS/TPP nanoparticles, Fourier transform infrared spectroscopy (FTIR), Atomic force microscopy (AFM), Loading efficiency

### I. INTRODUCTION

Krill oil (KO) is a rich alternative source of polyunsaturated fatty acids (PUFAs) besides algal and fish oil mainly of which are docosahexaenoic acid (DHA) and eicosapentaenoic acid (EPA) (Bustos, Romo, Yáñez, Díaz, & Romo, 2003). DHA and EPA have recently gained a significant attention for their use as nutritional supplements, functional foods and pharmaceutical ingredients (Yao, Xiao, & McClements, 2014). The dietary intake of DHA and EPA, particularly from Western life style diet, is considerably lower than recommended levels and their conversion from precursor  $\alpha$ -linolenic acid (ALA) in the body is also far from to cover up the deficit (Burdge & Calder, 2005). KO also has a significant level of other constituents (200-400 ppm) such as various potent antioxidants and astaxanthin (provitamin E) (Kolakowska, Kolakowski, & Szczygielski, 1994). The unique phospholipids (naturally rich in omega-3 fatty acids and diverse antioxidants) profile of KO offers a wide range of benefits as compared with usual fish oil. It highly facilitates the absorptive passage of fatty acids through epithelium, increasing bioavailability and improving the  $\Omega$ -3: $\Omega$ -6 fatty acids ratio (Schuchardt & Hahn, 2013; Werner, Havinga, Kuipers, & Verkade, 2004). EPA, DHA and astaxanthin are highly unsaturated in their nature and prone to degradation. KO fortified sea food products are even more susceptible to undergo the oxidation degradation as compared to those which are enriched with other n-3 rich oil (Pietrowski, Tahergorabi, Matak, Tou, & Jaczynski, 2011). PUFAs rapidly oxidized products at trace level can produce off flavour and other quality disadvantages within the food products. This rationale bases the foundation for development of a delivery system that may enhance its solubility in water as well as minimize oxidation at the same time for future use of KO in food applications.

Stabilising through micro-encapsulation seems to be a reasonable approach that enables the successful incorporation of PUFAs into a wide variety of food products (Barrow, Nolan, & Jin, 2007). To protect the core

loaded bioactive compounds from the harsh environmental conditions, polymeric nanoparticles development as encapsulants or "shell" is being implemented in the food industry as well as many other related industries (Acosta, 2009; Chen, Remondetto, & Subirade, 2006; Duclairoir, Orecchioni, Depraetere, Osterstock, & Nakache, 2003; Guterres, Alves, & Pohlmann, 2007; Jang & Lee, 2008; Pinto Reis, Neufeld, Ribeiro, & Veiga, 2006; Rothenfluh, Bermudez, O'Neil, & Hubbell, 2008). A two-step emulsion and ionic-gelation method has been reported to synthesize chitosan (CS) nanoparticles which are non-toxic, organic solvent free and convenient for targeted delivery of bioactive compounds (Malafaya, Silva, & Reis, 2007; Yang et al., 2011). This method was based on the principle of ionic interactions between the positively charged primary amino groups of CS and the negatively charged groups of polyanion such as sodium tripolyphosphate (TPP; the most extensively used ion cross-linking agent) (Shu & Zhu, 2002).

Traditional time consuming gas chromatography and gravimetric analysis have been used widely to determine the oil contents in variety of samples by many researchers (Aziz, Gill, Dutilleul, Neufeld, & Kermasha, 2014; Indarti, Majid, Hashim, & Chong, 2005; Liu, Low, & Nickerson, 2010; Ulberth & Henninger, 1992). But these methods considered being time consuming, invasive, indirect and involving the use of hazardous solvents that is not environment friendly. Therefore, an alternative quantification method based on Fourier transform infrared (FTIR) spectroscopy has been employed in this study. FTIR spectroscopy has gained much popularity for its use in many researches as a quantitative tool owing to its rapid and non-destructive nature, simple sample preparation, ease of use and less or no solvent consumption for monitoring quality (Anzanello, Fogliatto, Ortiz, Limberger, & Mariotti, 2014; Blanco, Valdés, Bayod, Fernández-Marí, & Llorente, 2004; Kondepati, Keese, Michael Heise, & Backhaus, 2006; Ortiz et al., 2013; Rodionova et al., 2005) as well as quantity of the raw materials (Hu, Erxleben, Ryder, & McArdle, 2010; Kumar, Tang, & Chen, 2008; Salari & Young, 1998). FTIR is an easy and fast quantitative method which provides reliable results of analysis. Previously, the technique has been applied quantitatively for various food systems to determine solid non-fat content in raw milk (Bassbasi, Platikanov, Tauler, & Oussama, 2014),  $\alpha$ -tocopherol in refined bleached and deodorized palm olein (Che Man, Ammawath, & Mirghani, 2005), fatty acid contents in microencapsulated fish oil supplement (Vongsivut et al., 2012a), sugar and organic acid contents (Bureau et al., 2009). Previously, FTIR has not been reported for the quantification of biodegradable CS/TPP nanoparticles loaded KO, hence keeping in view the above mentioned rationale(s) in this current study we aimed to develop a simple, an inexpensive and rapid method for quantification of KO loaded in CS/TPP nanoparticles.

## II. MATERIALS AND METHODS

### 2.1 MATERIALS

Antarctic krill oil containing ~40 % phospholipid, ~28-30 %  $\Omega$ -3 fatty acids and  $\leq 200$  mg kg<sup>-1</sup> astaxanthin (claimed by manufacturer) was purchased from Hutai Biopharm Inc. Sichuan, China. Partially deacetylated crab shell derived chitosan (CS; degree of deacetylation; 91.5 %;  $M_w$ : 100 kDa) was obtained from Golden-Shell Biochemical Co., Ltd. Hangzhou, China. Tween 80, Glacial acetic acid, Sodium tripolyphosphate (TPP) and rest of all chemicals used in this study were of analytical grade and purchased from Sinopharm Chemical Reagent Co., Ltd., China.

### 2.2 KO-LOADED CS/TPP NANOPARTICLES PREPARATION

KO loaded CS/TPP nanoparticles were prepared following the method described elsewhere with slight modifications (Calvo & Remunan-Lopez, 1997) and (Hosseini, Zandi, Rezaei, & Farahmandghavi, 2013). Briefly, 1.5 % (w/v) CS solution was prepared by agitating CS in 1% v/v aqueous acetic acid solution at ambient temperature for 24 hrs. The solution was centrifuged at 8000 rpm for 20 min and supernatant was filtered using 0.8  $\mu$ m filter paper. Tween 80 (0.5g) was added as a surfactant to the CS solution (40 mL) and the mixture was stirred at 45 °C for 2 hrs till complete homogenization. 0.6 g KO was gradually poured into aqueous CS solution and subsequently the system was homogenized twice using an Ultra-Turrax (T25, Ika-Werke, Staufen, Germany) at a speed of 13,000 rpm for 1 min and 16,500 for 2 min, respectively. Same volume of TPP solution (40 mL) was added drop by drop to the O/W emulsion and agitated for 40 min. The particles formed were collected by centrifugation at 10,000  $\times$ g for 30 min at 20 °C and washed several times with dd H<sub>2</sub>O to remove excess of KO. Wet particles were dispersed in distilled water (25 mL) and suspensions were immediately freeze-dried at -35 °C for 72 hrs to obtain powder samples. Powder samples were stored in dry conditions at 25 °C.

### 2.3 GRAVIMETRIC ANALYSIS

#### 2.3.1 EXTRACTION OF TOTAL OIL

Extraction of total oil was done using the method of Zhang et al. (Klinkesorn, Sophanodora, Chinachoti, Decker, & McClements, 2006) with some modifications. Briefly, 0.5 g particles were agitated with 5 mL water for 15 min. The resulting solution was then extracted with 25 mL hexane/isopropanol (3:1, v/v) and agitation

was executed for 15 min. The solution was centrifuged for another 15 min at 8000×g. The clear organic phase was carefully withdrawn while the aqueous phase was re-extracted with the solvent mixture (Heinzelmann, Franke, Velasco, & Márquez-Ruiz, 2000). After filtration through anhydrous sodium sulfate, the solvent was evaporated in a rotary evaporator (RE-52AA, Shanghai Biochemical Instrument Company, China) at 70 °C. The solvent-free extract was dried at 105 °C until a constant weight reached and the amount of encapsulated oil was determined gravimetrically. The loading capacity was calculated using Eq. (I).

$$LC (\%) = \frac{\text{Total amount of loaded KO}}{\text{Weight of nanoparticles after lyophilization}} \times 100 \quad (\text{I})$$

## 2.4 FOURIER TRANSFORM INFRAREDSPECTROSCOPY

Infrared spectra of all samples were obtained using Nicolet iS10, FTIR spectrometer equipped with KBr accessory (Thermo Fisher Scientific Inc., USA). For spectral acquisition, a film of each liquid sample (~2 µL) deposited on a KBr disk. Solid sample of 1 mg was taken in 99 mg KBr to prepare pellet. The mixture was condensed in 13 mm die at a pressure 5 tons for 1 min. The pellets were scanned spectra were obtained using 16 scans at a resolution of 4 cm<sup>-1</sup> over the frequency range of 4000-400 cm<sup>-1</sup>. All the spectra were recorded using Nicolet OMNIC software (Version 8.2)

## 2.5 ATOMIC FORCE MICROSCOPY

Bruker Dimension Icon atomic force microscopy (Bruker AXS, Germany) in ScanAsyst mode was employed to record the image of CS/TPP nanoparticles and KOloaded CS/TPP nanoparticles using silicon tip (TESP, Bruker, nom. Freq. 320 kHz, nom. Spring constant of 42 N/m). A drop of nanoparticle suspension (0.05 mg/mL) deposited on freshly cleaved mica surface and air dried overnight at 25 °C. Deflection and height mode image, both were obtained simultaneously at a fixed scan rate frequency of 0.997 Hz (resolution of 512×512 pixels in 5×5 µm dimensions). All images analysed using Digital NanoScope Analysis software (version 1.40, Bruker Corporation) and presented in zero order two-dimensional flattening.

## 2.6 FTIR CALIBRATIONS

Measured amounts of CS and KO were mixed for standard calibration curve. Lyophilized CS and KO mixture ranging from 0.005 mg to 1.5 mg in oven dried KBr were prepared to formulate uniform 100 g pellets. All the standards spectra were analysed in Essential FTIR software v3.50.059 (Operant LLC) to plot a calibration model.

## 2.7 FTIR SPECTRA PROCESSING AND METHOD DEVELOPMENT

Quantification of KO embedded in nanoparticles was carried determined by FTIR following the method described by Reig et al. 2002 (Reig, Adelantado, & Moya Moreno, 2002) based on Beer-Lambert law and the principle of constant ratio. Essential FTIR software v3.10.016 was used for the computation (Operant LLC). Based on the constant ratio method, the quantity of the standard mixtures or nanoparticles which were mixed or added to KBr had no effect on the ratio between the selected peaks. Nevertheless, KO is in liquid state this procedure did not require special liquid cuvette with the fixed path length. Instead, the common solid holder with KBr disc was utilised and found to be reliable. In this study, the interference between CS/TPP nanoparticles and KO peaks was minimised by selecting the absorption peaks for each material that appeared to be minimally interfered by the other materials. This was performed by comparing the spectra of all the raw materials as shown in Fig. 1. Furthermore, the interference between CS/TPP nanoparticles and KO was minimised by selecting the ratio  $A_{KO}/A_{CS/TPP \text{ nanoparticles}}$  and assigned it to be the “quantitative response” for this method. Selected peaks are shown in Table 1 and Fig. 2.

The predictive values were calculated by the software based on Beer-Lambert law which can be further interpreted in this study based on the following Eq. II.

$$\left( \frac{A_{KO} - A_{KO \text{ baseline}}}{A_{CSNPs} - A_{CSNPs \text{ baseline}}} \right) = \text{Slope} \cdot \frac{KO}{CSNPs} + \text{Constant} \quad (\text{II})$$

Repeatability test, relative standard deviation (RSD), was performed by taking 6 repeated FTIR scans for the standard mixture KO:CS/TPP nanoparticles 1:1. The predicted quantitative response,  $A_{Koil} / A_{CS/TPP \text{ nanoparticles}}$ , was calculated for each scan to determine RSD.

Limit of detection (LOD) and limit of quantification (LOQ) were calculated based on the following Eqs. III and IV, respectively:

$$LOD = 3.3 \frac{\sigma}{S} \quad (\text{III})$$

$$LOQ = 10 \frac{\sigma}{S} \quad (\text{IV})$$

Where:  $\sigma$  and S are standard deviations of the response and the slope, respectively.

After plotting standard curves,  $R^2$  and RSD values were compared between the selected peaks (Table 1) in order to choose the best calibration curve as a reference for KO quantification from nanoparticles, the best curve was characterized by  $R^2$  closest to 1 and the lowest RSD.

### III. RESULTS AND DISCUSSION

#### 3.1 FOURIER TRANSFORM INFRARED SPECTROSCOPIC ANALYSIS

Fabrication material used in this study and formation of KO loaded in CS/TPP nanoparticles was characterized by FTIR. The major IR absorption bands of CS spectrum were attributed to O–H ( $3451\text{ cm}^{-1}$ ), C–H ( $2876\text{ cm}^{-1}$ ), C–O stretch ( $1647\text{ cm}^{-1}$ ) and N–H stretching vibration of amide II at  $1588\text{ cm}^{-1}$  (Fig. 1A). In the TPP spectrum, two intense absorption bands were found. The peaks in the range of  $1220\text{--}1080\text{ cm}^{-1}$  attributed to P=O stretching and at  $899\text{ cm}^{-1}$  to P–O along with P–O–P (Rodrigues, da Costa, & Grenha, 2012) (Fig. 1B).

With incorporation of TPP in CS the peak of  $3421\text{ cm}^{-1}$  becomes wider indicating that the hydrogen bonding is enhanced. Also, in the TPP spectra the peak at  $1212\text{ cm}^{-1}$  which indicates P=O stretch, appeared in the CS/TPP nanoparticles spectra at  $1218\text{ cm}^{-1}$  as a result of the cross-linking between CS and TPP. Finally, in the spectra of the nanoparticles the peaks for N–H bending vibration of amine I at  $1598\text{ cm}^{-1}$  and the amide II carbonyl stretch at  $1654\text{ cm}^{-1}$  shifted to  $1568\text{ cm}^{-1}$  and  $1630\text{ cm}^{-1}$ , respectively. These results indicate the interaction between amino groups of CS and phosphate groups of TPP. We may conclude that the appearing of these peaks is an indication of nanoparticle formation and inter- as well as intra-molecular actions are enhanced in CS/TPP nanoparticles (Bhumkar & Pokharkar, 2006; De Moura et al., 2009; De Pinho Neves et al., 2014; Xu & Du, 2003) (Fig. 1C).

Further, we confirmed the incorporation of KO in CS/TPP nanoparticles by FTIR via comparing with characteristic peaks in the KO spectra. On the other hand, the increase in CH stretching peak intensity at  $2869\text{--}2974\text{ cm}^{-1}$  reflects the location of KO in the CS matrix. These results were further strengthened as the increase in CH stretching peak intensity was observed with increasing KO content. Therefore, we can consider CH stretching as a strong indicator of KO encapsulation in any matrix (Vongsvivut et al., 2012b; Zhao, Wei, Liu, & Liu, 2014). Thus, emulsion and later electrostatic interaction of CS with TPP, a two-step process successfully encapsulated KO in CS/TPP nanoparticles. The results confirmed the presence of KO with specific peaks at  $3416\text{ cm}^{-1}$  (OH),  $3012\text{ cm}^{-1}$  (=C–H stretching),  $3000\text{--}2800\text{ cm}^{-1}$  (C–H stretching),  $1740\text{ cm}^{-1}$  (C=O stretching band),  $1465\text{ cm}^{-1}$  (–CH<sub>2</sub>– bending),  $1379\text{ cm}^{-1}$  (–CH<sub>3</sub> bending),  $1091\text{ cm}^{-1}$  (CO stretching),  $971\text{ cm}^{-1}$  (C=C stretching band) as shown in (Fig. 1D, E and Fig. 2).

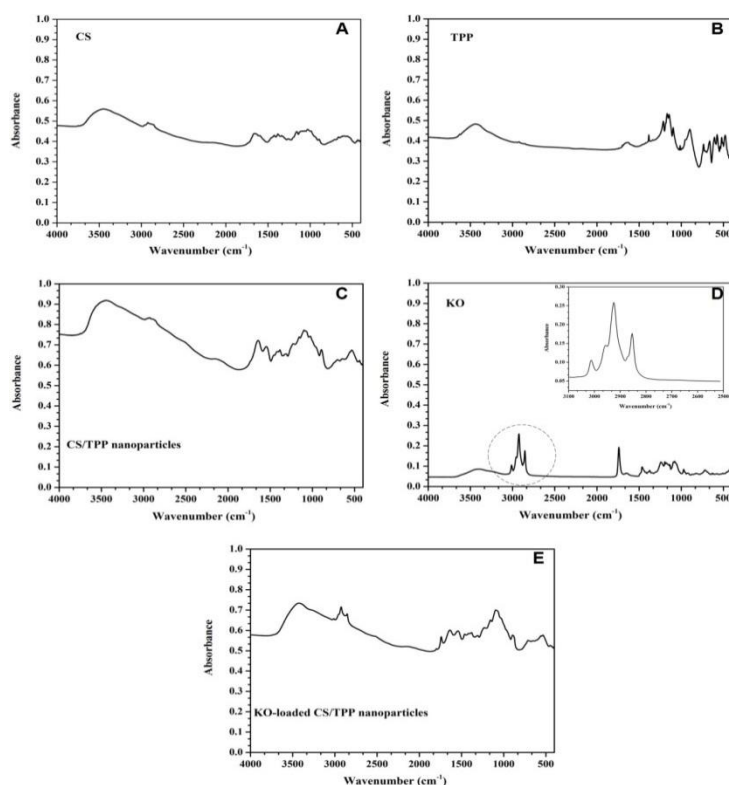
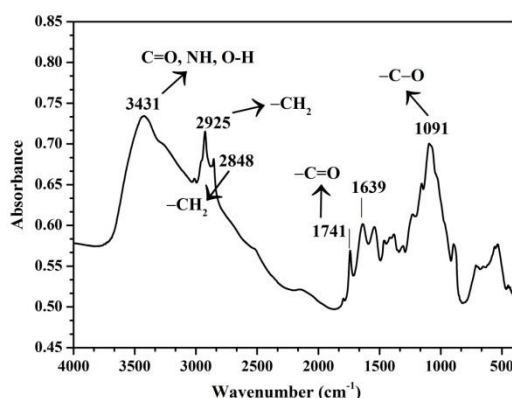


Figure 1: FTIR spectra of the raw materials used in nanoparticles fabrication.



**Figure 2:** Selected peaks from FTIR spectrum of KOloaded CS/TPP nanoparticles at 1:1 ratio.

### 3.2 ATOMIC FORCE MICROSCOPY ANALYSIS

The surface morphology of the particles was observed by atomic force microscopy (AFM) imaging. The AFM images of the CS/TPP nanoparticles demonstrate regular distribution and spherical shape that appear to be well separated and stable over the steps of the preparation process (**Fig. 3A and B**). Next we continue to investigate the KOloaded CS/TPP nanoparticles. AFM imaging has revealed aggregation that due to the presence of remaining KO around the particles (**Fig. 3C and D**).

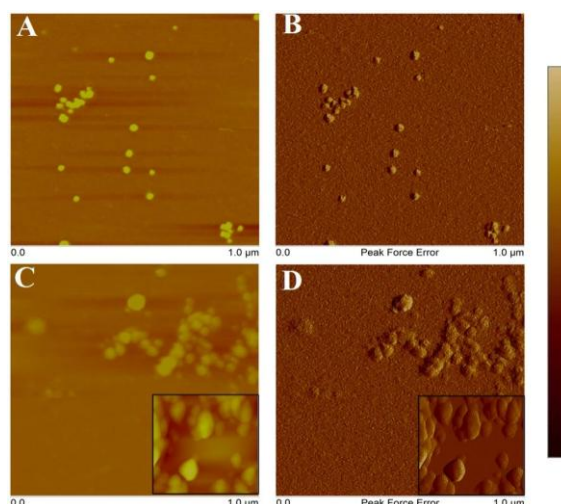


**Figure 3:** (A and B) AFM images showing the surface morphology of CS/TPP nanoparticles; (C and D) KOloaded CS/TPP nanoparticles (C, D). (A, C are height images; B, D are deflection images). The colorscale on the right side is 100 nm.

### 3.3 STANDARD CURVE CONSTRUCTION

Quantification of KO was based on Beer-Lambert law and constant ratio method (Reig et al., 2002). Absorbance peaks were selected with minimal interference from the other components by comparing the spectra of the raw materials (**Fig. 4**). Consequently, peak selection was made mainly by comparing the FTIR spectra of CS/TPP nanoparticle and KO and their mixture as shown in **Fig. 1 and 2**. The two distinct peaks at about 2925  $\text{cm}^{-1}$  and 2848  $\text{cm}^{-1}$  were selected for KO. For CS/TPP nanoparticle, peak at 1741  $\text{cm}^{-1}$  and 1091  $\text{cm}^{-1}$  were chosen. Different mathematical combinations of the peak's heights and the baseline regions were tested in order to obtain the best standard curve (**Table 1 and Fig. 4**).

Based on **Table 1**, the best standard curve was obtained at the absorbance 2925  $\text{cm}^{-1}$  with the baseline correction at 1845 – 1898  $\text{cm}^{-1}$  for KO, and the absorbance 1091  $\text{cm}^{-1}$  with baseline correction at 1845–1898  $\text{cm}^{-1}$  for CS/TPP nanoparticle (**Fig. 4D**). At these range of wavelength, the  $R^2$  and the RSD values are the closest to 1 (0.99) and the lowest (1.075%), respectively.

**Table 1:** Selected peaks from FTIR spectra of the KO and CS/TPP nanoparticles standard mixtures in order to construct the best standard curve LOD and LOQ are represented by % (w/w)KO/CS-TPP nanoparticles.

KO peak (cm <sup>-1</sup> )			CS/TPP nanoparticles peaks (cm <sup>-1</sup> )			R2	RSD (%)	LOD	LOQ	Figure
Region	Peak	Baseline	Region	Peak	Baseline					
2866-2875	2848	2455-2550	1704-1765	1741	1845-1898	0.9431	3.037	3.56	10.80	Fig. 4A
2896-2946	2925	1845-1898	1704-1765	1741	1845-1898	0.9689	2.793	2.70	8.18	Fig. 4B
2866-2875	2848	2455-2550	1086-1099	1091	1845-1898	0.9826	1.531	1.78	5.39	Fig. 4C
2896-2946	2925	1845-1898	1086-1099	1091	1845-1898	0.9959	1.075	1.24	3.77	Fig. 4D

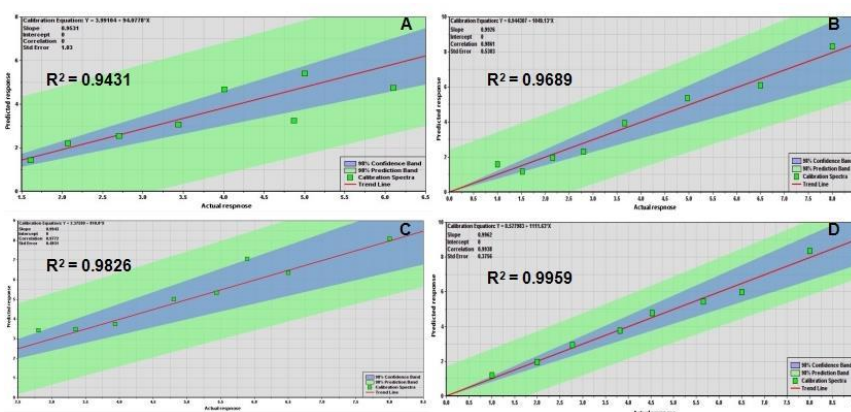


**Figure 4:** Standard curves obtained from FTIR spectra based on Beer- Lambert law. Each curve represents a set of selected peaks explained in Table 1.

### 3.4 QUANTIFICATION OF KO IN KO-LOADED CS/TPP NANOPARTICLES

FTIR spectrum of CS/TPP nanoparticles (Fig. 1) was used to quantify the loading efficiency of KO. Using the abovementioned best standard curve (Fig. 4D), KO loading efficiency was estimated to be  $22.2 \pm 0.26$  % using FTIR method and it was  $23.8 \pm 0.07$  %, when estimated gravimetrically. The study recommends the use of FTIR as a quantitative analytical tool for PUFA supplements to avoid sample preparation complexity and time consumption. The most impressive thing is that once the initial calibration curve is set up, the analysis is extremely rapid and simple with no accuracy issues.

## IV. CONCLUSION

Quantification of KO in nanoparticles by means of FTIR is a rapid and easy approach to apply. Acquisition of FTIR spectral data directly from the KO loaded CS/TPP nanoparticles, a good linear calibration curve ( $R^2 = 0.9959$ ) was achieved. The FTIR spectroscopic technique is advantageous over gravimetric method due to rapid spectral data collection directly from original KO loaded CS/TPP nanoparticles without any sample pre-treatment. Further, technique is also environmentally friendly and very cost effective since there is no other solvent or chemical, besides the samples, involved in the process of the analysis. The method will help to accelerate and improve the characterisation of KO nanoparticles during development and optimization stage.

## ACKNOWLEDGEMENT

The authors declare no conflict of interest. This work was financially supported by NSFC 31571891 and 31401533; JUSRP 51507 and 11422; 111Project B07029 and PCSIRT0627.

## REFERENCES

- [1]. Acosta, E. (2009). Bioavailability of nanoparticles in nutrient and nutraceutical delivery. *Current Opinion in Colloid & Interface Science*, 14(1), 3–15.
- [2]. Anzanello, M. J., Fogliatto, F. S., Ortiz, R. S., Limberger, R., & Mariotti, K. (2014). Selecting relevant Fourier transform infrared spectroscopy wavenumbers for clustering authentic and counterfeit drug samples. *Science & Justice: Journal of the Forensic Science Society*, 54(5), 363–8.
- [3]. Aziz, S., Gill, J., Dutilleul, P., Neufeld, R., & Kermasha, S. (2014). Microencapsulation of krill oil using complex coacervation. *Journal of Microencapsulation*, 31(8), 774–784.
- [4]. Barrow, C. J., Nolan, C., & Jin, Y. (2007). Stabilization of highly unsaturated fatty acids and delivery into foods. *Lipid Technology*, 19(5), 108–111.
- [5]. Bassbasi, M., Platikanov, S., Tauler, R., & Oussama, A. (2014). FTIR-ATR determination of solid non fat (SNF) in raw milk using PLS and SVM chemometric methods. *Food Chemistry*, 146, 250–4.
- [6]. Bhumkar, D. R., & Pokharkar, V. B. (2006). Studies on effect of pH on cross-linking of chitosan with sodium tripolyphosphate: A technical note. *AAPS PharmSciTech*, 7(2), E138–E143.

- [7]. Blanco, M., Valdés, D., Bayod, M., Fernández-Marí, F., & Llorente, I. (2004). Characterization and analysis of polymorphs by near-infrared spectrometry. *Analytica Chimica Acta*, 502(2), 221–227.
- [8]. Burdge, G. C., & Calder, P. C. (2005). Conversion of alpha-linolenic acid to longer-chain polyunsaturated fatty acids in human adults. *Reproduction, Nutrition, Development*, 45(5), 581–97.
- [9]. Bureau, S., Ruiz, D., Reich, M., Gouble, B., Bertrand, D., Audergon, J.-M., & Renard, C. M. G. C. (2009). Application of ATR-FTIR for a rapid and simultaneous determination of sugars and organic acids in apricot fruit. *Food Chemistry*, 115(3), 1133–1140.
- [10]. Bustos, R., Romo, L., Yáñez, K., Díaz, G., & Romo, C. (2003). Oxidative stability of carotenoid pigments and polyunsaturated fatty acids in microparticulate diets containing krill oil for nutrition of marine fish larvae. *Journal of Food Engineering*, 56(2-3), 289–293.
- [11]. Calvo, P., & Remunan-Lopez, C. (1997). Novel hydrophilic chitosan-polyethylene oxide nanoparticles as protein carriers. *Journal of Applied Polymer Science*, 63(1), 125–132.
- [12]. Che Man, Y. B., Ammawath, W., & Mirghani, M. E. S. (2005). Determining  $\alpha$ -tocopherol in refined bleached and deodorized palm olein by Fourier transform infrared spectroscopy. *Food Chemistry*, 90(1-2), 323–327.
- [13]. Chen, L., Remondetto, G. E., & Subirade, M. (2006). Food protein-based materials as nutraceutical delivery systems. *Trends in Food Science & Technology*, 17(5), 272–283.
- [14]. De Moura, M. R., Aouada, F. A., Avena-Bustillos, R. J., McHugh, T. H., Krochta, J. M., & Mattoso, L. H. C. (2009). Improved barrier and mechanical properties of novel hydroxypropyl methylcellulose edible films with chitosan/tripolyphosphate nanoparticles. *Journal of Food Engineering*, 92(4), 448–453.
- [15]. De Pinho Neves, A. L., Milioli, C. C., Müller, L., Riella, H. G., Kuhnen, N. C., & Stulzer, H. K. (2014). Factorial design as tool in chitosan nanoparticles development by ionic gelation technique. *Colloids and Surfaces A: Physicochemical and Engineering Aspects*, 445, 34–39.
- [16]. Duclairroir, C., Orecchioni, A.-M., Depraetere, P., Osterstock, F., & Nakache, E. (2003). Evaluation of gliadins nanoparticles as drug delivery systems: a study of three different drugs. *International Journal of Pharmaceutics*, 253(1-2), 133–144.
- [17]. Guterres, S. S., Alves, M. P., & Pohlmann, A. R. (2007). Polymeric nanoparticles, nanospheres and nanocapsules, for cutaneous applications. *Drug Target Insights*, 2, 147–57.
- [18]. Heinzelmann, K., Franke, K., Velasco, J., & Márquez-Ruiz, G. (2000). Microencapsulation of fish oil by freeze-drying techniques and influence of process parameters on oxidative stability during storage. *European Food Research and Technology*, 211(4), 234–239.
- [19]. Hosseini, S. F., Zandi, M., Rezaei, M., & Farahmandghavi, F. (2013). Two-step method for encapsulation of oregano essential oil in chitosan nanoparticles: Preparation, characterization and in vitro release study. *Carbohydrate Polymers*, 95(1), 50–56.
- [20]. Hu, Y., Erxleben, A., Ryder, A. G., & McArdle, P. (2010). Quantitative analysis of sulfathiazole polymorphs in ternary mixtures by attenuated total reflectance infrared, near-infrared and Raman spectroscopy. *Journal of Pharmaceutical and Biomedical Analysis*, 53(3), 412–20.
- [21]. Indarti, E., Majid, M. I. A., Hashim, R., & Chong, A. (2005). Direct FAME synthesis for rapid total lipid analysis from fish oil and cod liver oil. *Journal of Food Composition and Analysis*, 18(2-3), 161–170.
- [22]. Jang, K.-I., & Lee, H. G. (2008). Stability of chitosan nanoparticles for L-ascorbic acid during heat treatment in aqueous solution. *Journal of Agricultural and Food Chemistry*, 56(6), 1936–41.
- [23]. Klinkesorn, U., Sophanodora, P., Chinachoti, P., Decker, E. a., & McClements, D. J. (2006). Characterization of spray-dried tuna oil emulsified in two-layered interfacial membranes prepared using electrostatic layer-by-layer deposition. *Food Research International*, 39(4), 449–457.
- [24]. Kolakowska, A., Kolakowski, E., & Szczygielski, M. (1994). Winter season krill (*Euphausia superba* D.) as a source of n-3 polyunsaturated fatty acids. *Food / Nahrung*, 38(2), 128–134.
- [25]. Kondepati, V. R., Keese, M., Michael Heise, H., & Backhaus, J. (2006). Detection of structural disorders in pancreatic tumour DNA with Fourier-transform infrared spectroscopy. *Vibrational Spectroscopy*, 40(1), 33–39.
- [26]. Kumar, S. A., Tang, C.-F., & Chen, S.-M. (2008). Electroanalytical determination of acetaminophen using nano-TiO<sub>2</sub>/polymer coated electrode in the presence of dopamine. *Talanta*, 76(5), 997–1005.
- [27]. Liu, S., Low, N. H., & Nickerson, M. T. (2010). Entrapment of flaxseed oil within gelatin-gum Arabic capsules. *JAOCS, Journal of the American Oil Chemists' Society*, 87(7), 809–815.
- [28]. Malafaya, P. B., Silva, G. a., & Reis, R. L. (2007). Natural-origin polymers as carriers and scaffolds for biomolecules and cell delivery in tissue engineering applications. *Advanced Drug Delivery Reviews*, 59(4-5), 207–233.
- [29]. Ortiz, R. S., Mariotti, K. de C., Fank, B., Limberger, R. P., Anzanello, M. J., & Mayorga, P. (2013). Counterfeit Cialis and Viagra fingerprinting by ATR-FTIR spectroscopy with chemometry: can the same pharmaceutical powder mixture be used to falsify two medicines? *Forensic Science International*, 226(1-3), 282–9.
- [30]. Pietrowski, B. N., Tahergorabi, R., Matak, K. E., Tou, J. C., & Jaczynski, J. (2011). Chemical properties of surimi seafood nutrified with  $\omega$ -3 rich oils. *Food Chemistry*, 129(3), 912–9.
- [31]. Pinto Reis, C., Neufeld, R. J., Ribeiro, A. J., & Veiga, F. (2006). Nanoencapsulation I. Methods for preparation of drug-loaded polymeric nanoparticles. *Nanomedicine: Nanotechnology, Biology, and Medicine*, 2(1), 8–21.
- [32]. Reig, F. B., Adelantado, J. V. G., & Moya Moreno, M. C. M. (2002). FTIR quantitative analysis of calcium carbonate (calcite) and silica (quartz) mixtures using the constant ratio method. Application to geological samples. *Talanta*, 58(4), 811–21.
- [33]. Rodionova, O. Y., Houmøller, L. P., Pomerantsev, A. L., Geladi, P., Burger, J., Dorofeyev, V. L., & Arzamastsev, A. P. (2005). NIR spectrometry for counterfeit drug detection. *Analytica Chimica Acta*, 549(1-2), 151–158.
- [34]. Rodrigues, S., da Costa, A.M.R., & Grenha, A. (2012). Chitosan/carrageenan nanoparticles: effect of cross-linking with tripolyphosphate and charge ratios. *Carbohydrate Polymers*, 89(1), 282-9.
- [35]. Rothenfluh, D. A., Bermudez, H., O'Neil, C. P., & Hubbell, J. A. (2008). Biofunctional polymer nanoparticles for intra-articular targeting and retention in cartilage. *Nature Materials*, 7(3), 248–54.
- [36]. Salari, A., & Young, R. E. (1998). Application of attenuated total reflectance FTIR spectroscopy to the analysis of mixtures of pharmaceutical polymorphs. *International Journal of Pharmaceutics*, 163(1-2), 157–166.
- [37]. Schuchardt, J. P., & Hahn, A. (2013). Bioavailability of long-chain omega-3 fatty acids. *Prostaglandins, Leukotrienes, and Essential Fatty Acids*, 89(1), 1–8.
- [38]. Shu, X., & Zhu, K. (2002). The influence of multivalent phosphate structure on the properties of ionically cross-linked chitosan films for controlled drug release. *European Journal of Pharmaceutics and Biopharmaceutics*, 54(2), 235–243.
- [39]. Ulberth, F., & Henninger, M. (1992). One-step extraction/methylation method for determining the fatty acid composition of processed foods. *Journal of the American Oil Chemists' Society*, 69(2), 174–177.

- [40]. Vongsivut, J., Heraud, P., Zhang, W., Kralovec, J. A., McNaughton, D., & Barrow, C. J. (2012a). Quantitative determination of fatty acid compositions in micro-encapsulated fish-oil supplements using Fourier transform infrared (FTIR) spectroscopy. *Food Chemistry*, 135(2), 603–9.
- [41]. Vongsivut, J., Heraud, P., Zhang, W., Kralovec, J. a., McNaughton, D., & Barrow, C. J. (2012b). Quantitative determination of fatty acid compositions in micro-encapsulated fish-oil supplements using Fourier transform infrared (FTIR) spectroscopy. *Food Chemistry*, 135(2), 603–9.
- [42]. Werner, A., Havinga, R., Kuipers, F., & Verkade, H. J. (2004). Treatment of EFA deficiency with dietary triglycerides or phospholipids in a murine model of extrahepatic cholestasis. *American Journal of Physiology. Gastrointestinal and Liver Physiology*, 286(5), G822–32.
- [43]. Xu, Y., & Du, Y. (2003). Effect of molecular structure of chitosan on protein delivery properties of chitosan nanoparticles. *International Journal of Pharmaceutics*, 250(1), 215–226.
- [44]. Yang, S.-J., Lin, F.-H., Tsai, H.-M., Lin, C.-F., Chin, H.-C., Wong, J.-M., & Shieh, M.-J. (2011). Alginate-folic acid-modified chitosan nanoparticles for photodynamic detection of intestinal neoplasms. *Biomaterials*, 32(8), 2174–2182.
- [45]. Yao, M., Xiao, H., & McClements, D. J. (2014). Delivery of lipophilic bioactives: assembly, disassembly, and reassembly of lipid nanoparticles. *Annual Review of Food Science and Technology*, 5, 53–81.
- [46]. Zhao, J., Wei, S., Liu, F., & Liu, D. (2014). Separation and characterization of acetone-soluble phosphatidylcholine from Antarctic krill (*Euphausia superba*) oil. *European Food Research and Technology*, 238, 1023–1028.